Online Estimation of State of Charge in Li-Ion Batteries Using Impulse Response Concept

Amir Hossein Ranjbar, *Student Member, IEEE*, Anahita Banaei, *Member, IEEE*, Amir Khoobroo, *Member, IEEE*, and Babak Fahimi, *Senior Member, IEEE*

***Abstract*—Lithium-ion batteries exhibit high levels of energy and power density among electrochemical batteries. These attributes make them suitable as the energy storage system in electric, hybrid electric vehicle, and plug-in vehicles (EV/HEV/PHEV). One of the important requirements in automotive batteries is to monitor their real time state-of-charge (SOC) and state-of-health (SOH). Open circuit voltage, as one parameter used for predicting the SOC in the battery, is not readily available during charge and discharge cycles. In this paper a new method for prediction of the terminal voltage in li-ion batteries based on the impulse response concept has been proposed. By obtaining the impulse response of the li-ion battery, one can use the terminal current to predict the output voltage of the battery. Online comparison of the predicted and measured terminal voltage provides a tool for online monitoring of the SOH and SOC.**

***Index Terms*—Impulse response, li-ion battery, state-of-charge (SOC).**

I. Introduction

INTEREST IN electric and hybrid electric vehicles (EV/HEV) and plug-in vehicles (PHEV) has grown in recent years in response to rising fuel costs and increased concerns about pollution. Energy storage system is the major unit in EV/HEVs and batteries are the primary option for the energy storage system. Hence, the demand for rechargeable batteries has witnessed an increase as well. The battery system choice is very crucial for EV/HEVs and it requires satisfying important characteristics like high performance and high reliability. While accelerating a hybrid vehicle a large amount of energy is required to be taken out of battery during a short period of time. So the battery not only needs to store a large amount of energy but also should be able to deliver considerable energy in a short time (high power). Li-ion batteries have high power density comparing to other chemistries and this property along with other advantages of this batteries make them the main contender for energy storage in EV/HEVs. Some of the capabilities of li-ion batteries are as follows:

- high energy density;
- high power density;
- low self-discharge;
- fast charging;
- high energy-to-weight ratio;
- no memory effect;
- durability if charged properly.

Achieving an efficient and reliable battery management system is an important key in EV/HEV development. Battery management systems monitor key operational parameters, such as current, voltage, temperature, state-of-charge (SOC) and state-of-health (SOH). Li-ion batteries are less tolerant of abuse than other battery chemistries, so they particularly require precise monitoring of charge and health status to ensure that no overcharging or undercharging is occurred and also it is capable to deliver the specific amount of charge. Hence, one of the important issues to be considered here is the prediction of state-of-charge (SOC) and state-of-health (SOH).

A wide variety of researches which have been done on the SOC estimation for the HEV batteries rely upon open circuit voltage of the battery [1]–[5]. These methods do not take into account parameter variations in electrochemical batteries and as such their accuracy is subject to the SOH of the battery, aging effects, and possible manufacturing imperfections. In addition, the open circuit voltage is not readily available while the batteries are in use. These methods are not accurate enough and as a result would jeopardize the chance of correct charging and the performance of the battery. This can potentially lead to thermal runway in li-ion batteries.

Another SOC estimation method is based on current integration during charge and discharge states of the battery [6]–[10]. However, the estimation error existed in each state integrates with the current and increases gradually. Measurement of the battery internal impedance or resistance is yet another method which again does not provide acceptable results [11]–[13]. Another approach for estimating SOC of a battery is to model the electrochemical dynamics of the battery and various processes taking place inside the cell, then using the model to predict the terminal voltage [14]–[19]. However measuring all the electrical and chemical parameters of a cell is a difficult task.

The present paper proposes a new method for online monitoring of the SOC by the virtue of the impulse response of the battery.

II. Fundamentals of Li-Ion Batteries and Battery Modeling Methods

A. Li-Ion Batteries

Lithium-ion batteries present a family of rechargeable batteries in which a lithium ion moves between anode and cathode during charge and discharge. Electrolyte consists of lithium salts

Manuscript received February 22, 2011; revised May 30, 2011; accepted June 24, 2011. Date of publication December 19, 2011; date of current version February 23, 2012. Paper no. TSG-00058-2011.

A. H. Ranjbar and B. Fahimi are with the University of Texas at Dallas, Richardson, TX (e-mail: axr106420@utdallas.edu; fahimi@utdallas.edu).

A. Banaei and A. Khoobroo are with the SynQor company, Garland, TX (e-mail: anahita_banaei@yahoo.com; amir.khoobroo@mavs.uta.edu).

Color versions of one or more of the figures in this paper are available online at http://ieeexplore.ieee.org.

Digital Object Identifier 10.1109/TSG.2011.2169818

such as $LiPF_6$, $LiPF_6$, or $LIClO_4$ to act as a carrier, conducting lithium ions between anode and cathode. A variety of materials can be used for anode and cathode, but most of the times anode is made of graphite and cathode is made of a lithium oxides such as $LiCoO_2$ and $LiMn_2O_4$. The typical reaction taking place in cathode is as follows:

$$LiCoO_2 \Leftrightarrow Li_{1-x}CoO_2 + xLi^+ + xe^- \tag{1}$$

the reaction in anode can be shown as below

$$xLi^+ + xe^- + 6C \Leftrightarrow Li_xC_6. \tag{2}$$

in which x denotes the number of lithium ions. One of the characteristics of li-ion batteries which stands out among other chemistries is that they have smaller internal leakage. An li-ion battery loses a small percentage of its charge comparing to other types of batteries within a given period of time. They are generally lighter than other types of batteries containing the same amount of energy. Further, it is notable that li-ion batteries do not have memory effect, which means there is no need to discharge them completely before recharging. All these advantages make them an excellent choice for electric and hybrid electric vehicles (EV/HEV).

It must be noted that li-ion batteries are sensitive to deep discharge or overcharge and these states of extremely high or too low SOC can lead to irreversible damage in the battery.

There are various methods to model a li-ion battery. The method used in the proposed method here is based on the impulse response of the battery.

B. Impulse Response Concept

For a pair of real functions which (i.e., f and g) are defined over a continuous interval of time the convolution of f and g is denoted by $f*g$ and the basic definition is given by

$$\begin{aligned}(f*g)(t) &= \int_{-\infty}^{+\infty} f(\tau)\ldots g(t-\tau)d\tau \\ &= \int_{-\infty}^{+\infty} f(t-\tau)\ldots g(\tau)d\tau.\end{aligned} \tag{3}$$

The convolution in discrete time domain is represented as follows:

$$\begin{aligned}(f*g)[n] &= \sum_{k=-\infty}^{+\infty} f[k].g[n-k] \\ &= \sum_{k=-\infty}^{+\infty} f[n-k]\ldots g[k].\end{aligned} \tag{4}$$

Another point to be made is that convolution is commutative, which means it does not matter which function is taken first.

From the linear system theory the output of a linear time invariant (LTI) system for an arbitrary input can be determined using its impulse response as shown below

$$y[k] = x[k]*h[k] \tag{5}$$

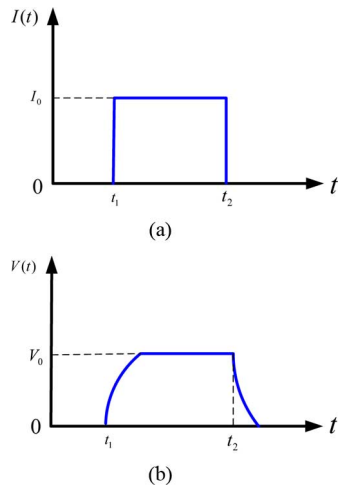

Fig. 1. Impulse response demonstration (a) Applied pulse of current (b) output voltage of the battery.

where $x[k]$, $h[k]$ and $y[k]$ are the input, impulse response, and output of the system respectively. In other words, the convolution of the input to the system with its impulse response gives the output of the system.

In order to determine the impulse response of a battery a narrow pulse of current is applied to the battery and the output voltage is monitored as shown in Fig. 1.

In order to obtain accurate result, an engineering approximation of the following definition should be chosen:

$$\delta(t) = \lim_{(t_2-t_1)\to 0} I(t)\Big|_{I_0\ldots(t_2-t_1)=1}. \tag{6}$$

This equation indicates that a current impulse is defined by a narrow pulse of current with the unity area. It is important to note that the width of the pulse should be sufficiently smaller than the shortest time constant of the system. Due to relatively large time constants of the electrochemical batteries a good compromise between the timing of the pulse and maximum magnitude of the waveform can be made. In order to define an impulse for a specific system, suppose a first order LTI system characterized as follows:

$$\frac{dy}{dt} + \frac{1}{\tau}y = x(t) \tag{7}$$

where y is the output, x is the input, and τ is the time constant of the system. Taking the Laplace transform, the transfer function of the system would be presented as

$$H(s) = \frac{\tau}{1+\tau.s}. \tag{8}$$

Suppose that the input of the system $(f(t))$ is defined as Fig. 2 which is characterized as

$$f(t) = \frac{1}{\Delta}(u(t) - u(t-\Delta)). \tag{9}$$

The Laplace transform of $(f(t))$ is calculated as follows:

$$F(s) = \frac{1}{\Delta.s}(1 - e^{-\Delta s}) \tag{10}$$

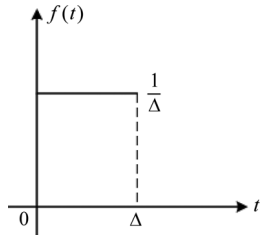

Fig. 2. A typical input for the system.

$$= \frac{1}{\Delta.s}\left[1-\left(1+(-\Delta.s)+\frac{(-\Delta.s)^2}{2!}+\frac{(-\Delta.s)^3}{3!}+\cdots\right)\right]. \tag{11}$$

$$= 1-\frac{\Delta.s}{2!}+\frac{(\Delta.s)^2}{3!}-\frac{(\Delta.s)^3}{4!}+\cdots \tag{12}$$

In order to find the response of the system to the input $f(t)$, $F(s)$ is multiplied by the transfer function of the system, $H(s)$, as shown in (13) at the bottom of the page.

To consider $f(t)$ as an impulse, the response of the system to $f(t)$ should be equal to the impulse response of the system

$$Y(s) = F(s).H(s) = H(s) = \frac{\tau}{1+\tau.s}. \tag{14}$$

This means that all the terms except the first one in (13) need to be zero

$$\frac{\Delta.s}{1+\tau.s} \to 0 \quad \Rightarrow \quad \Delta \ll \tau. \tag{15}$$

Therefore, if Δ is much smaller than the time constant of the system, $f(t)$ can be assumed as an approximation for impulse function for the system.

To further quantify the width of the current pulse (i.e., Δ) to develop a good approximation of $f(t)$ (as an impulse input to the system) the first two terms in (13) are considered and the remaining terms are assumed to be sufficiently small and therefore negligible. It is assumed that the second term can be ignored if its contribution to the time domain response is smaller than 10% of the total response, which means

$$Y(s) = \frac{\tau}{1+\tau.s} - \frac{\tau}{2!}\times\left(\frac{\Delta.s}{1+\tau.s}\right) \overset{L^{-1}}{\longrightarrow} \tag{16}$$

$$y(t) = \tau.e^{-\tau.t} - \frac{\tau.\Delta}{2!}(-\tau.e^{-\tau.t})$$

$$\tau.e^{-\tau.t} < 10\% \times \left(\tau.e^{-\tau.t} - \frac{\tau.\Delta}{2!}(-\tau.e^{-\tau.t})\right) \tag{17}$$

$$1 < 0.1 \times \left(1+\frac{\tau.\Delta}{2}\right) \tag{18}$$

$$20 < 2+\tau.\Delta \tag{19}$$

$$18 < \tau.\Delta. \tag{20}$$

This computation provides a more clear understanding on the required inequality of (15). In fact knowing the smallest time constant of the system (i.e., battery) will allow us to select the pulse current such that a good approximation of the impulse response is achieved.

Assuming a linear time invariant behavior within the reasonable window of time, the impulse response of a battery can be used as a battery model. This model can then be used, along with the real time measurement of the current, to calculate the output voltage. Having the impulse response of the battery and convolving it with measured input current to the battery the output voltage can be calculated. This can be shown as follows:

$$\nu[k] = i[k]*h[k] \tag{21}$$

where $i[k]$, $h[k]$, and $\nu[k]$ are the battery terminal current, impulse response of the battery, and the terminal voltage respectively.

C. ARMAX Modeling

Autoregressive moving average models (ARMAX) can be used to express the impulse response of a discrete time LTI system numerically. For a single-input/single-output system (SISO), the ARMAX polynomial model structure is given by

$$A(q)y(t) = B(q)u(t) + C(q)e(t) \tag{22}$$

where $y(t)$ represents the output at time $\boldsymbol{t}$, $u(t)$ represents the input at time $\boldsymbol{t}$, $e(t)$ is the white-noise disturbance and q^{-1} is the back-shift operator. Also

$$A(q) = 1 + a_1q^{-1} + \cdots + a_nq^{-n} \tag{23}$$

$$B(q) = b_1 + b_2q^{-1} + \cdots + b_mq^{-m} \tag{24}$$

$$C(q) = 1 + c_1q^{-1} + \cdots + a_rq^{-r} \tag{25}$$

where $\boldsymbol{n}$, $\boldsymbol{m}$, and $\boldsymbol{r}$ are the orders of the polynomials, respectively [20]. The appropriate model orders should be determined in order to estimate the ARMAX model. Having specified the model (i.e., the transfer function formed by $A(.)$ and $B(.)$ polynomials), the input current of the battery can be used to compute the output voltage (i.e., $y(t)$).

D. Equivalent Circuit Modeling

The battery equivalent circuit is a commonly used method for modeling of a battery. It provides a model to explain the voltage

$$Y(s) = F(s).H(s) = \frac{\tau}{1+\tau.s}\times\left[1-\frac{\Delta.s}{2!}+\frac{(\Delta.s)^2}{3!}-\frac{(\Delta.s)^3}{4!}+\cdots\right]$$
$$= \left[\frac{\tau}{1+\tau.s}-\frac{\tau}{2!}\times\left(\frac{\Delta.s}{1+\tau.s}\right)+\frac{\tau(\Delta.s)}{3!}\times\left(\frac{\Delta.s}{1+\tau.s}\right)-\frac{\tau(\Delta.s)^2}{4!}\times\left(\frac{\Delta.s}{1+\tau.s}\right)+\cdots\right] \tag{13}$$

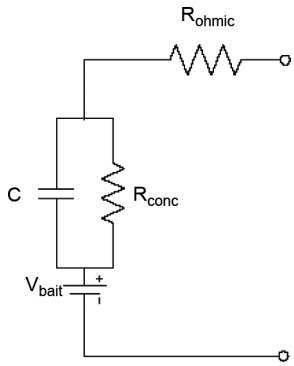

Fig. 3. Equivalent circuit of a rechargeable battery.

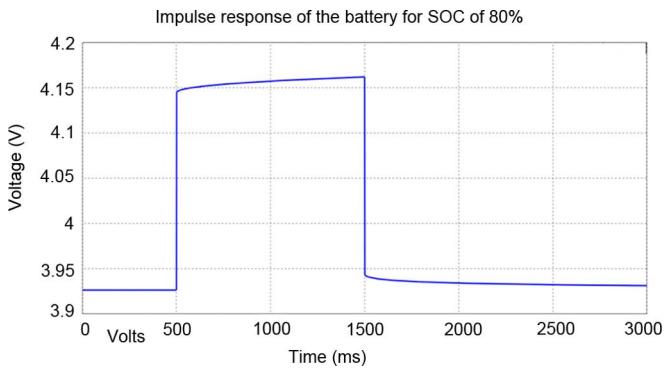

Fig. 4. Impulse response of 18650 li-ion battery, SOC=80%.

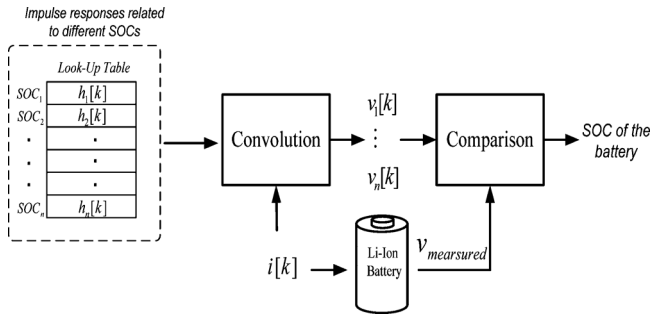

Fig. 5. Block diagram of the proposed method.

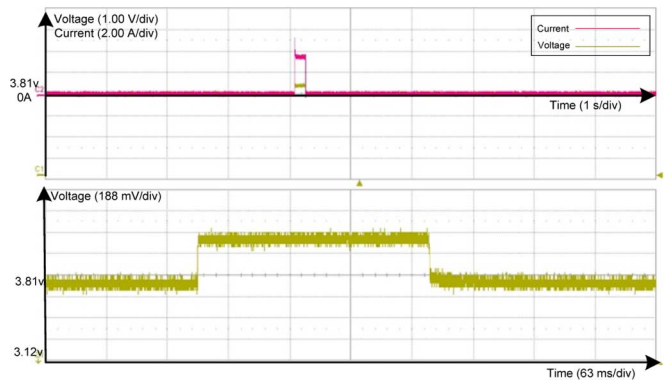

Fig. 6. Impulse response of 18650 li-ion battery, SOC = 75%.

waveforms and to quantify the results into four circuit parameters which represent various parts of the battery. There are various configurations for the equivalent circuit model [21]. Fig. 3 shows a typical equivalent circuit for a rechargeable battery.

$R_{\rm ohmic}$ represents the electrode and packaging resistance of the battery, $R_{\rm conc}$ represents the battery's internal resistance, which defines the maximum current a battery can deliver and accounts for charging and discharging losses. C is the capacity of a battery which is formed by series connection of the double layer capacitance formed by each pair of battery cells and is indicative of the finite amount of electric charge stored inside the battery. $V_{\rm batt}$ represents the battery's rated voltage at no-load (open circuit) condition. To obtain various parameters of the model some charging and discharging tests need to be made [22].

III. Method Description

The method used in this paper for modeling a li-ion battery is based on the impulse response of the battery. The impulse response, at a known temperature, is dependent upon the amount of charge that is left in the battery or in other words to its state-of-charge (SOC). Different levels of SOC imply different impulse responses [23]. It must be noted that the term impulse inherently suggests that the duration of the current pulse is significantly smaller than the smallest time constant in the system. Fig. 4 shows the impulse response of the 18650 li-ion battery for state-of-charge of 80%.

A family of impulse responses for various levels of SOC is calculated and stored in a look-up table. In other words, the whole available range of SOC of the battery is being partitioned by i individual levels each corresponding to a specific impulse response $(h_i[k])$. Notably the input current applied to the battery and the battery output voltage to that specific current are available experimentally. Having the impulse response of the battery stored in a look-up table, the terminal voltage for a measured input current over a known interval of time can be calculated by convolution of the measured current with all the impulse responses stored in the look-up table. So, for an arbitrary input a set of $\boldsymbol{n}$ output voltages can be achieved as follows:

$$\nu_i[k] = i[k]*h_i[k] \Rightarrow \nu_i[k] = \sum_{j=1}^{N} i[j]*h_i[k-j]. \qquad (26)$$

Comparing the measured output voltage and the calculated voltages using the impulse responses from the look-up table, the proper impulse response related to the battery would be determined. The selected impulse response projects the least error between the measured and calculated voltages. As the SOC corresponding to each impulse response is known, the state-of-charge of the battery can be determined. Fig. 5 shows the block diagram of the proposed method.

IV. Experimental Results

In this paper two types of li-ion batteries have been used for experimental verification: battery No. 1, which is 18650 li-ion battery and the capacity is 2.2 Ah; and battery No. 2, which is 26650 li-ion battery and the capacity is 3 Ah. The experiments have been done in room temperature, 25 °C. Figs. 6 and 7 show different impulse responses of the No. 1 battery for state-of-charges of 75% and 20%. Figures show that the results are different for various levels of state-of-charge.

The idea has been verified by simulation results using Battery Design Studio V13.6. A charging current pulse with magnitude of 1 A and width of 1 s is applied to the 18650 li-ion battery

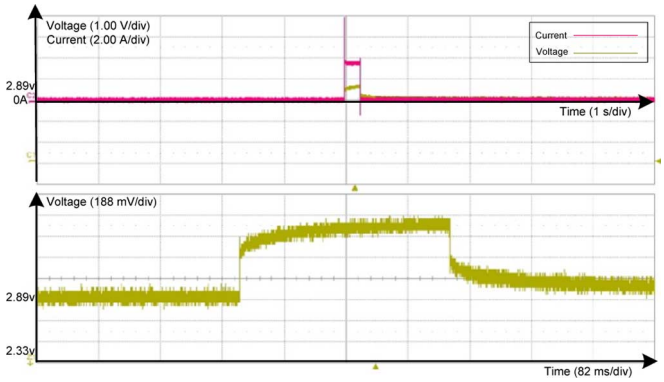

Fig. 7. Impulse response of 18650 li-ion battery, SOC = 20%.

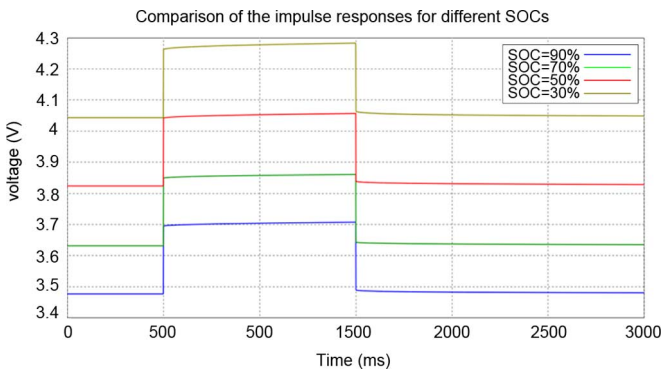

Fig. 8. Comparison of the calculated impulse responses for applying the charging current pulse of 1 A for various SOCs: 30%, 50%, 70%, and 90%.

model. This test has been done for a variety of state-of-charges and, as it is shown in Fig. 8, different responses are achieved.

It must be noted that the impulse response is also related to the magnitude of current applied to the battery in each level of SOC. So for estimating the impulse response a specific current pulse is chosen for all different state of charges. Fig. 9 shows voltage responses to different current values of 0.5 A, 1 A, and 1.5 A while SOC = 80%.

The impulse response of the battery can be represented using an ARMAX model. As mentioned previously the multivariable ARMAX model is shown as below

$$\begin{aligned} &A_0 \times y(t) + A_1 \times y(t-T) \\ &\quad + \cdots + A_n \times y(t-nT) \\ &= B_0 \times u(t) + B_1 \times u(t-T) \\ &\quad + \cdots + B_m \times u(t-mT) + e(t). \end{aligned} \tag{27}$$

Coefficients would be determined based on the current and voltage input waveforms used for impulse response calculation. Using the experimental data, the impulse response of the battery is represented as follows:

$$y(t) = B_0 \times u(t) + B_1 \times u(t-T) + \cdots + B_m \times u(t-mT) + e(t). \tag{28}$$

The impulse responses of the battery corresponding to different state-of-charges are calculated using the system identification toolbox in MATLAB v7.6. Furthermore, a discharging current of 2.2 A for 10 s is applied to the battery No. 2 (26650 li-ion) while the SOC is 100%, 60%, and 20%. Fig. 10 shows

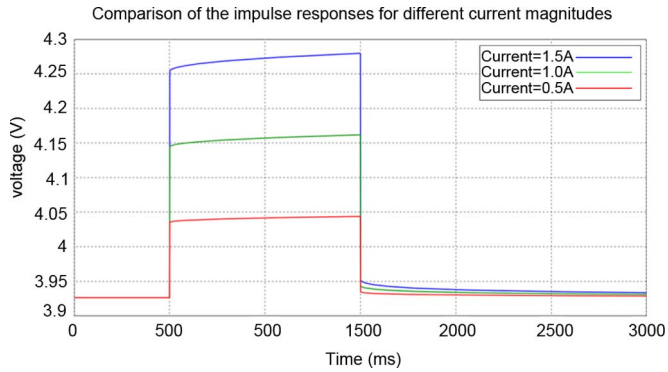

Fig. 9. Comparison of the calculated impulse responses for applying various charging pulses with duration of 1 s and current magnitudes of: 0.5 A, 1.0 A, and 1.5 A, SOC = 80%.

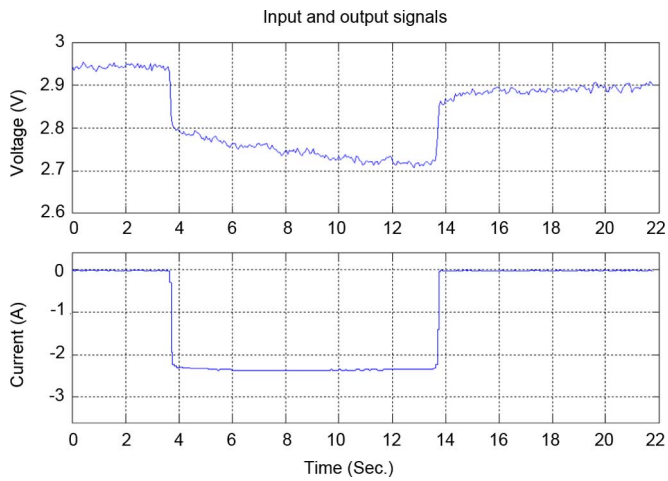

Fig. 10. Applied input current and measured output voltage of the battery No. 2 for 10 s, SOC = 20%.

the applied current and measured output voltage of the battery for SOC of 20%.

Using the current and voltage waveforms in Fig. 10, the impulse response of the battery under test is estimated for SOC of 20%. Impulse responses corresponding to other values of SOC are calculated by the same method. The estimated impulse response of the battery for SOC of 60% is shown in Fig. 11. The coefficients of the impulse response is stored and convolved by any current input to form the output voltage of the battery with the SOC of 60%.

To validate the proposed method, the calculated impulse responses corresponding to different state-of-charges need to be validated and their convolution results need to be compared to the real data measured from the battery. A pulse of 2.3 A current is applied to the 26650 li-ion battery (battery No. 2) and the output voltage waveform is measured and stored. The same current waveform is convolved with the impulse responses of the battery for three various state-of-charges (20%, 60%, and 100%). Then, the results of the convolutions are compared to the measured voltage of the battery in order to determine the minimum error and the maximum match to the real data.

Fig. 12 shows the comparison of measured output voltage of the battery No. 1 (26650 li-ion) to the calculated output voltages using various impulse responses corresponding to different state-of-charges. As shown in this figure, data calculated by the

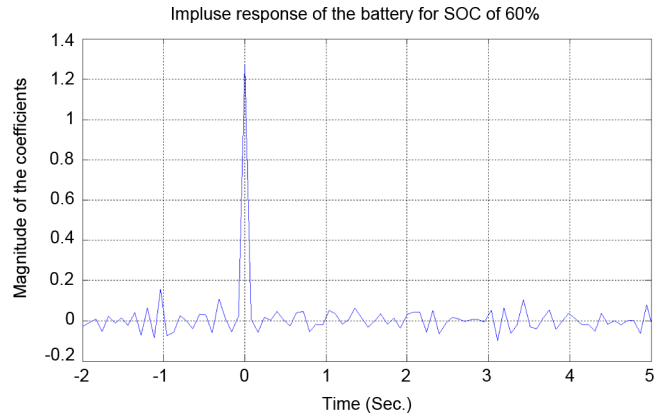

Fig. 11. Calculated impulse response of the battery No. 2, SOC = 60%.

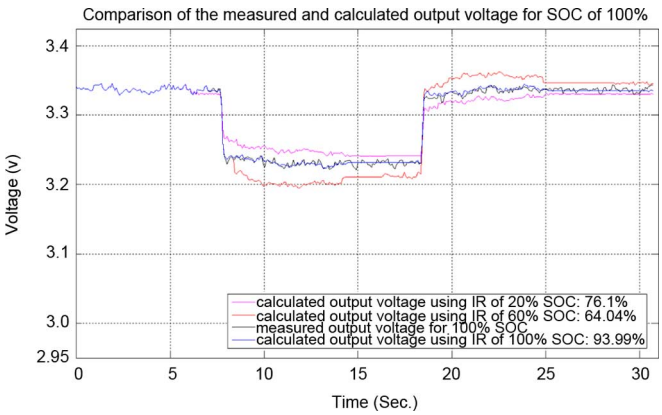

Fig. 12. Comparison of measured output voltage of the battery No. 2 with SOC of 100% with the calculated output voltages using IR for SOCs of 100%, 60%, and 20%.

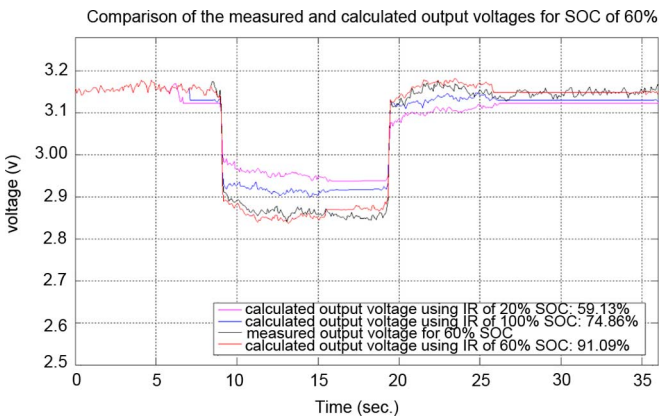

Fig. 13. Comparison of measured output voltage of the battery No. 2 with SOC of 60% with the calculated output voltages using IR for SOCs of 100%, 60%, and 20%.

impulse response corresponding to SOC of 100% has the best fit to the measured data (94%), whereas the other two impulse responses corresponding to SOCs of 60% and 20% have low fitting percentage (76% and 64% respectively).

The fitness (%) is based on the mean square error between the measured data and the simulated output of the model

$$E = \frac{1}{n}\sum_{i=1}^{n}\left(\frac{Y_i - \hat{Y}_i}{Y_i}\right)^2$$
$$Fit(\%) = (1 - E) \times 100 \tag{29}$$

where Y_i and $\hat{Y}_i$ are the measured and calculated data samples and n is the number of the samples. One hundred percent corresponds to a perfect fit (no error) and 0% corresponds to a model which is not capable of estimating any variation of the output.

Fig. 13 compares the measured output voltage of the battery for SOC of 60% to the calculated output voltages using various impulse responses corresponding to state-of-charges of 100%, 60%, and 20%. The calculated data using the impulse response of the battery for the SOC of 60% fits best to the real data (91.1%) compared to the calculated data using other impulse responses (75% of fitting for SOC of 100% and 59% of fitting for SOC of 20%).

In Fig. 14 the measured voltage of the battery with SOC of 20% for applying a discharge current of 2.5 A for 10 s is compared to the calculated output voltages using impulse responses of various SOCs of 100%, 60%, and 20%. Fig. 15 shows the same comparison as Fig. 14, but this time the comparison is for the results of applying two discharging cycles of 5 s and 15 s. It is obvious that the impulse response corresponding to 20% of SOC results in higher accuracy comparing to the other two impulse responses for SOCs of 100% and 60%.

The sensitivity of the fitness function is related to the current and voltage measurement errors. Using (29) the relationship of the Fitness value to the measured current and voltage is expressed as

$$E = \frac{1}{n}\sum_{i=1}^{n}\left(\frac{Y_i - \hat{Y}_i}{Y_i}\right)^2 = \frac{1}{n}\sum_{i=1}^{n}\left(\frac{Y_i - \sum_{j=1}^{m} I_{i-j}\cdot h_j}{Y_i}\right)^2. \tag{30}$$

Suppose α is the percentage of measurement error for current and β is the percentage of measurement error for voltage. Then the values of current and voltage change according to the following equations:

$$I_i = I_i \pm \alpha.I_i \tag{31}$$
$$Y_i = Y_i \pm \beta.Y_i. \tag{32}$$

Based on the error percentage of current and voltage values, the corresponding error would be reflected on the Fitness percentage. Table I represents the possible current sensor accuracies and their corresponding effect on the fitness values. Table II shows the effect of various voltage measurement errors on the fitness percentage. Fig. 16 depicts the absolute values of fitness errors versus the absolute values of measurement errors.

V. Conclusion

This paper presents an online method for prediction of the terminal voltage in li-ion batteries which is based on the use of convolution theory. The impulse response of the battery is captured for various levels of state-of-charge (SOC). For a given (measured) input current the output voltage is calculated by convolving it with the appropriate set of impulse responses. Comparison of the calculated voltages with the measured output

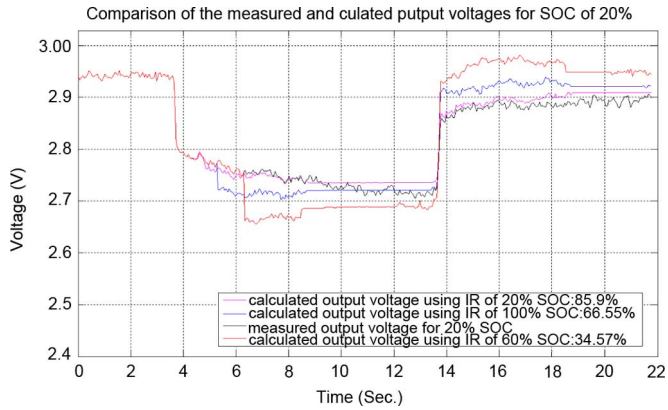

Fig. 14. Comparison of measured output voltage of the battery No. 2 with SOC of 20% with the calculated output voltages using IR for SOCs of 100%, 60%, and 20%.

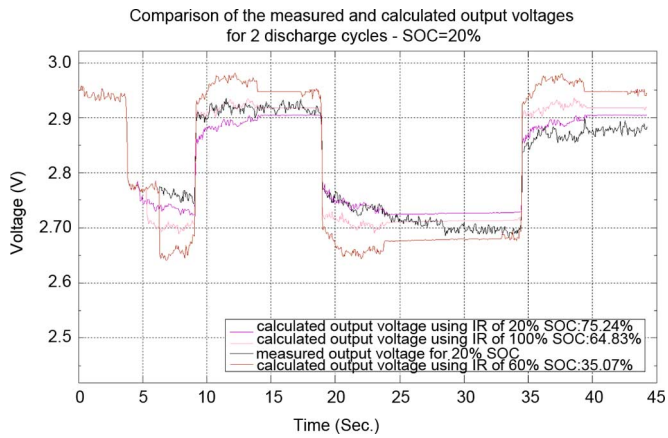

Fig. 15. Comparison of measured output voltage of the battery No. 2 with SOC of 20% for 2 discharging cycles with the calculated output voltages using three various impulse responses.

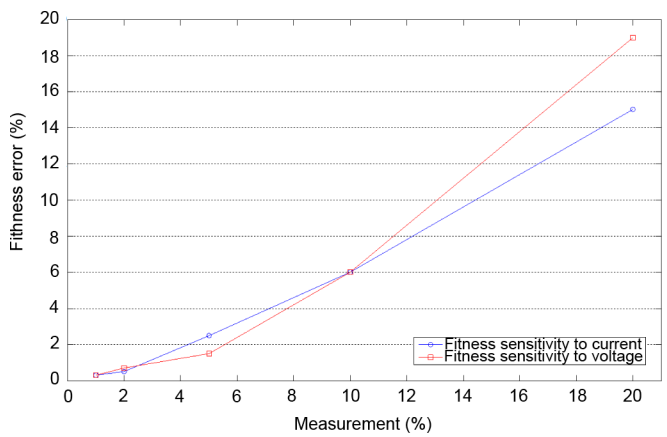

Fig. 16. The fitness error versus current and voltage measurement error (absolute values).

voltage from terminals of the battery creates a method to estimate the state-of-charge of the battery.

Using simulation and experimental tests, claims of the proposed method have been verified. From Figs. 11–13, it can be seen that calculated voltage corresponding to the proper SOC illustrates the best fit to the real data measured from battery.

TABLE I
THE SENSITIVITY OF FITNESS VALUE TO THE CURRENT MEASUREMENT ERROR

Current Sensor Accuracy	Fitness Error
± 1%	± 0.3%
± 2%	± 0.5%
± 5%	± 2.5%
± 10%	± 6%
± 20%	± 15%

TABLE II
THE SENSITIVITY OF FITNESS VALUE TO THE VOLTAGE MEASUREMENT ERROR

Voltage Sensor Accuracy	Fitness Error
± 1%	± 0.3%
± 2%	± 0.7%
± 5%	± 1.5%
± 10%	± 6%
± 20%	± 19%

This method can be used as the key element for on-line charge monitoring of batteries in EVs and HEVs. The proposed method can be modified for other types of battery chemistries and various temperatures. It can also be used for detection of faults in the battery.

REFERENCES

[1] A. Szumanowski and Y. Chang, "Battery management system based on battery nonlinear dynamics modeling," *IEEE Trans. Veh. Tech.*, vol. 57, no. 3, pp. 1425–1432, 2008.

[2] B. Tsenter, "Battery management for hybrid electric vehicle and telecommunication applications," in *Proc. IEEE 17th Annu. Battery Conf. Appl. Adv.*, 2002, pp. 233–237.

[3] K. S. Ng, C. S. Moo, Y. P. Chen, and Y. C. Hsieh, "State-of-charge estimation for lead-acid batteries based on dynamic open-circuit voltage," in *Proc. IEEE 2nd Int. Power Energy Conf. (PECon)*, Dec. 2008, pp. 972–976.

[4] J. Chiasson, "Estimating the state of charge of a battery," in *Proc. IEEE Amer. Control Conf.*, Jun. 2003, vol. 4, pp. 2863–2868.

[5] S. Bogosyan, M. Gokasan, and D. J. Goering, "A novel model validation and estimation approach for hybrid serial electric vehicles," *IEEE Trans. Veh. Technol.*, vol. 56, no. 4, pp. 1485–1497, 2007.

[6] V. Pop, H. J. Bergveld, P. H. L. Notten, and P. P. L. Regtien, "Smart and accurate state-of-Charge indication in portable applications," in *Proc. IEEE Int. Conf. Power Electron. Drives Syst. (PEDS'05)*, vol. 1, pp. 262–267.

[7] K. Kutluay, Y. Cadirci, Y. S. Ozkazanc, and I. Cadirci, "A new online state-of-charge estimation and monitoring system for sealed lead-acid batteries in telecommunication power supplies," *IEEE Trans. Ind. Electron.*, vol. 52, no. 5, pp. 1315–1327, Oct. 2005.

[8] O. Caumont, P. L. Moigne, C. Rombaut, X. Muneret, and P. Lenain, "Energy gauge for lead-acid batteries in electric vehicles," *IEEE Trans. Energy Conversion*, vol. 15, no. 3, pp. 354–360, Sep. 2000.

[9] X. Wang and T. Stuart, "Charge measurement circuit for electric vehicle batteries," *IEEE Trans. Aerosp. Electron. Syst.*, vol. 38, no. 4, pp. 1201–1209, Oct. 2002.

[10] D. T. Lee, S. J. Shiah, C. M. Lee, and Y. C. Wang, "State-of-Charge estimation for electric scooters by using learning mechanisms," *IEEE Trans. Veh. Technol.*, vol. 56, no. 2, pp. 544–556, 2007.

[11] K. Onda, M. Nakayama, K. Fukuda, K. Wakahara, and T. Araki, "Cell impedance measurement by Laplace transformation of charge or discharge current-voltage," *J. Electrochem. Soc*, vol. 153, no. 6, pp. A1012–A1018, 2006.

[12] J. H. Kim, S. J. Lee, J. M. Lee, and B. H. Cho, "A new direct current internal resistance and state of charge relationship for the li-ion battery pulse power estimation," in *Proc. IEEE 7th Int. Conf. Power Electron. (ICPE'07)*, vol. 52, pp. 1173–1178.
[13] D. V. Do, C. Forgez, K. E. K. Benkara, and G. Friedrich, "Impedance observer for a li-ion battery using kalman filter," *IEEE Trans. Veh. Technol.*, vol. 58, no. 8, pp. 3930–3937, 2009.
[14] P. M. Gomadam, J. W. Weidner, R. A. Dougal, and R. E. White, "Mathematical modeling of lithium-ion and nickel battery systems," *J. Power Sources*, vol. 110, pp. 267–284, 2002.
[15] P. Shi, C. Bu, and Y. Zhao, "The ANN models for SOC/BRC estimation of li-ion battery," in *IEEE Int. Conf. Inf. Acquisition*, 2005, pp. 560–564.
[16] R. E. Garcia, Y. M. Chiang, W. C. Carter, P. Limthongkul, and C. M. Bishop, "Microstructural modeling and design of rechargeable lithium-ion batteries," *J. Electrochem. Soc*, vol. 152, no. 1, pp. A255–A263, 2005.
[17] S. Santhanagopalan and R. E. White, "State of charge estimation for electrical vehicle batteries," in *Proc. IEEE Int. Conf. Control Appl. (CCA)*, Sep. 2008, pp. 690–695.
[18] O. Barbarisi, R. Canaletti, L. Glielmo, M. Gosso, and F. Vasca, "State of charge stimator for NiMH batteries," in *Proc. 41th IEEE Conf. Decision Control*, Dec. 2002, vol. 2, pp. 1739–1744.
[19] A. M. C. Paz, J. M. Acevedo, J. D. Gandoy, and A. D. R. Vazquez, "Multisensor fibre optic for electrolyte density measurement in lead-acid batteries," in *Proc. IEEE 32nd Annu. Conf. Ind. Electron. (IECON)*, Nov. 2006, pp. 3012–3017.
[20] H. Yang, C. M. Huang, and C. L. Huang, "Identification of ARMAX model for short term load forecasting:An evolutionary programming approach," *IEEE Trans. Power Syst.*, vol. 11, no. 1, pp. 403–408, 1996.
[21] C. R. Gould, C. M. Bingham, D. A. Stone, and P. Bentley, "New battery model and state-of-Health determination through subspace parameter estimation and state-observer techniques," *IEEE Trans. Veh. Technol.*, vol. 58, no. 8, pp. 3905–3916, 2009.
[22] M. Ragsdale, J. Brunet, and B. Fahimi, "A novel battery identification method based on pattern recognition," in *IEEE Int. Conf. Veh. Power Propulsion (VPPC'08)*, pp. 1–6.
[23] A. Banaei, A. Khoobroo, and B. Fahimi, "Online detection of terminal voltage in li-ion batteries via battery impulse response," in *IEEE Int. Conf. Veh. Power Propulsion (VPPC)*, Sep. 2009, pp. 194–198.

Amir Hossein Ranjbar received the B.S. degree from Babol University of Technology, Babol, Iran, in 2006 and the M.S. degree in electrical engineering from Amirkabir University of Technology (Tehran Polytechnic), Tehran, Iran, in 2009, where he was honored as the first rank among the graduate students. He is currently working toward the Ph.D degree and Research Assistant at Renewable Energy and Vehicular Technology (REVT) laboratory at the University of Texas at Dallas (UTD).

He was also the Executive Director of Iranian Association of Electrical and Electronics Engineers (IAEEE) from 2007 to 2009. He is currently a Research Assistant at REVT, UTD. His research interests include reliability analysis of power electronics systems, application of power electronics in microgrids, electrical machines, and drives.

Anahita Banaei (M'07) received the B.Sc. degree in computer engineering from the University of Tehran, Iran, in 2002, the M.Sc. degree in electrical engineering from Isfahan University of Technology, Iran, in 2006, and the Ph.D. degree in electrical engineering from the University of Texas at Arlington in 2010.

She has coauthored 5 journal and conference papers in the general area of energy storage, battery management systems for electric and hybrid electric vehicles, and computer architecture. She also has one pending U.S. patent.

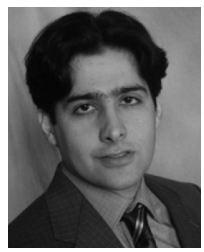

Amir Khoobroo (M'07) received the B.Sc. degree in electrical engineering from Sharif University of Technology, Iran, in 2003, the M.Sc. degree in electrical engineering from Isfahan University of Technology, Iran, in 2006, and the Ph.D. degree in electrical engineering from the University of Texas at Arlington in 2010.

He has coauthored 4 journal and 10 conference papers in the general area of adjustable speed motor drives and power electronics. He also has one pending U.S. patent.

Babak Fahimi (S'96–M'99–SM'02) received the Ph.D. in electrical engineering from Texas A&M University, College Station, in 1999.

He is currently a Professor of Electrical Engineering and the Director of the Renewable Energy and Vehicular Technology (REVT) Laboratory at the University of Texas at Dallas. He has coauthored over 190 scientific peer reviewed articles in prestigious journals and conference proceedings in the field of adjustable speed motor drives and power electronics. He has authored 15 book chapters, five technical reports, and has given numerous technical talks and tutorials on various aspects of design and control for adjustable speed drives and power electronic circuits over a wide range of applications. He holds four U.S. patents and has seven more pending.

Dr. Fahimi has been recognized by IEEE Richard M. Bass young power electronics investigator award in 2003, Office of Naval Research young investigator award in 2004, the IEEE TRANSACTIONS ON INDUSTRY APPLICATIONS Society best paper prize in 2006, Society of Automotive Engineering Ralph Teetor Educational Award in 2008, and Fulbright Scholarship in 2011 for his excellence in research and education. He has supervised 8 Ph.D. dissertations and 14 M.S. theses to completion. Three of his former Ph.D. students are assistant professors in academia. He has been the principal investigator of several successful projects funded by the NSF, DOE, ONR, and industry. He has been the general chairman of the IEEE Vehicle Power and Propulsion Conference in 2007, general chairman of the IEEE Applied Power Electronics and Expo in 2010, chairman of the electric machines committee in IEEE Industrial Electronics Society (2008–2010), chairman of the IEEE Future Energy Challenge (2009), Chairman of the Power Electronics Technical Committee in the IEEE Industrial Electronics Society (2011-present). He has been an associate editor for the IEEE TRANSACTIONS ON VEHICULAR TECHNOLOGY, the IEEE TRANSACTIONS ON POWER ELECTRONICS, the IEEE TRANSACTIONS ON INDUSTRIAL ELECTRONICS, and the IEEE TRANSACTIONS ON ENERGY CONVERSION. He has been the guest editor of several special sections of the IEEE TRANSACTIONS ON VEHICULAR TECHNOLOGY and the IEEE TRANSACTIONS ON INDUSTRIAL ELECTRONICS. He is a member of SAE.